ALL-FIBER APPROACH TO LONG-TERM STABLE TIMING DISTRIBUTION SYSTEM

M. Xin*, K. Şafak, F. X. Kärtner, CFEL, DESY, Hamburg, Germany
P. T. Callahan, M. Y. Peng, F. X. Kärtner, MIT, Cambridge, Massachusetts, USA

Abstract

A complete fiber-optic, high-precision, long-term stable timing distribution system is demonstrated over a 3.5-km polarization-maintaining fiber link for synchronization of next generation X-ray free-electron lasers. The residual timing jitter at [1 Hz, 1 MHz] is below 0.7 fs, and the RMS drift (<1 Hz) is 3.3 fs over 200 hours of continuous operation. This all-fiber-optic implementation will greatly reduce the complexity of optical alignment in timing distribution and improve the overall mechanical and timing stability of the system.

INTRODUCTION

Next generation FELs, such as the European XFEL [1] in Hamburg and Linac Coherent Light Source II [2] in Stanford, are predicted to deliver X-ray pulses shorter than 10 fs. Unlocking the high temporal-resolution capabilities of these facilities will require extremely stable timing distribution systems [3, 4] delivering better than 10-fs precision between optical and radio frequency (RF) sources located over kilometer distances. Over the past decade, we have been advancing a pulsed-optical timing distribution system [5-7] that uses the ultralow-noise pulse train from a mode-locked (master) laser as its timing signal. The timing signal is transferred through timing-stabilized fiber links from a central location to multiple end stations, where efficient and robust synchronization is realized using balanced optical cross-correlators (BOC) [8] for optical sources and balanced optical-microwave phase detectors [7] for RF sub-systems. Real facilities such as FLASH and the European XFEL need fiber networks consisting of 20 or more timing links, which require tremendous attention to the alignment and stability of the free-space optics to minimize timing-drifts induced by beam pointing instabilities. This situation also necessitates preamplification of the master laser's output to overcome excessive free-space to fiber coupling losses to provide adequate power for all timing links. To eliminate free-space optics and its disadvantages from the timing distribution system, we have developed integrated, fiber-coupled balanced optical cross-correlators (FC-BOC) using periodically-poled $KTiOPO_4$ (PPKTP) waveguides [9, 10]. These waveguides exhibit second harmonic (SH) conversion efficiencies up to 1.02 % / [W·cm^2] (20 times higher than the bulk optical devices), which will decrease the power demand from the master laser and consequently support more timing links. Furthermore, the robustness and ease of implementation of these fiber-coupled devices will eliminate alignment-related problems observed in free-space optics. In this paper, we present an all-fiber implementation of the pulsed-optical timing distribution system using FC-BOCs.

EXPERIMENTAL SETUP

A diagram of the experimental setup is shown in Fig. 1(a). The master laser operates at 1554-nm center wavelength with +22.4-dBm average output power, 150 fs pulse width and 216.66-MHz repetition rate. Its repetition rate is locked to a RF synthesizer (RF-S) to reduce the timing drift below 10 Hz. The only free-space part built in this experiment is the initial power separation elements comprised of one polarization beam splitter (PBS) and 3 half-wave plates. Furthermore, polarization-maintaining (PM) fiber components are chosen over standard single-mode (SM) fiber for the construction of the setup, as previous results obtained with SM fiber has showed substantial polarization-mode-dispersion effects in the out-of-loop link stabilization measurements [3]. After the PBS, the output of the master laser is coupled into two separate fiber paths: the out-of-loop reference path and the link stabilization unit. The out-of-loop reference path is a 1-m long PM fiber serving as the reference arm for the out-of-loop FC-BOC. The link stabilization unit starts with a fiber-coupled polarization beam splitter (FC-PBS1) which divides the optical power further into two segments. The first segment (traveling to the right through FC-PBS1 in Fig. 1(a)) is directed into the timing link which consists of a fiber-coupled faraday rotator (FC-FR), a fiber-coupled motorized delay line (FC-MD) with 560-ps range, a PM fiber stretcher (PM-FS), and a 3.5-km PM dispersion-compensated fiber spool (PM-DCF). The second segment is sent into a 0.5-m fiber having a fiber-coupled faraday mirror (FC-FM) at the end. The FC-FM turns the polarization of the pulses by $\pi/2$ upon reflection and guides them into the in-loop FC-BOC to serve as the reference pulses for the timing stabilization of the 3.5-km link.

Both of the two FC-BOCs are PPKTP waveguide chips in fiber-coupled packages with internal temperature control [10]. A schematic of the module is shown in Fig. 1(b). The wavelength division multiplexer (WDM) consists of a fiber-coupled dichroic beam-splitter cube coupling the input pulses into the waveguide for cross-correlation and separates the SH return path from the fundamentals. The forward and backward SH signals are then fed to the ports of a fiber-coupled BPD (FC-BPD).

* ming.xin@desy.de

ISBN 978-3-95450-134-2

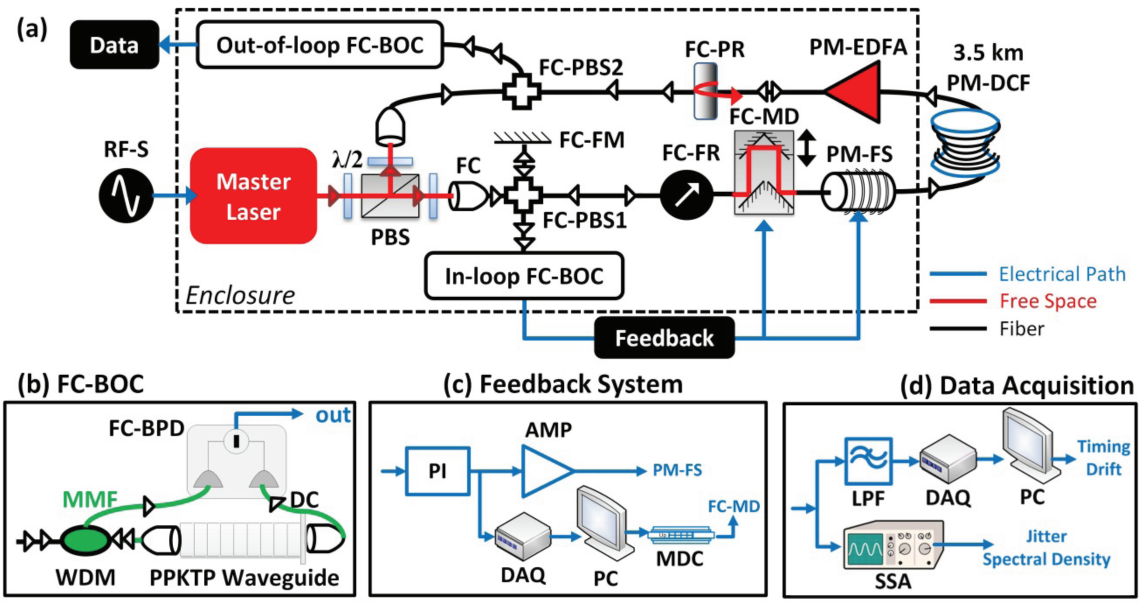

Figure 1: (a) Schematic of the link stabilization experiment. (b) Main elements the FC-BOCs. (c) Feedback system employed for the link delay compensation. (d) Data acquisition elements for the evaluation of the out-of-loop measurement results. Abbreviations: RF-S, RF synthesizer; FC, fiber coupler; FC-PBS, FC polarization beam splitter; FC-FM, FC faraday mirror; FC-FR, FC faraday rotator; FC-MD, FC motorized delay; PM-FS, PM fiber stretcher; PM-DCF, PM dispersion-compensated fiber; PM-EDFA, PM erbium doped fiber amplifier; FC-PR, fiber-coupled partial reflector; WDM, wavelength division multiplexer; MMF, multi-mode fiber; DC, dichroic coating; FC-BPD, fiber-coupled BPD; PI, proportional-integral controller; AMP, voltage amplifier; DAQ, data acquisition card with 1-Hz sampling rate; PC, personal computer; MDC, motorized delay controller; LPF, 2-Hz low-pass filter; SSA: Agilent 5052a signal source analyzer.

Power management of the fiber links is critical: high link output power is desirable for high signal-to-noise ratio, while low link operating power is needed to avoid fiber nonlinearity-induced timing errors. As a precaution, the fibers are operated with a maximum power of +13 dBm to avoid significant fiber nonlinearities. The input power to the timing link is set to +8 dBm such that after forward propagation, the link transmission loss results in +0-dBm link power. Custom-built bi-directional PM erbium doped fiber amplifier (PM-EDFA) is used in the last section of the timing link to boost the output power to +13 dBm. +3 dBm of power is reflected back by the fiber-coupled partial reflector (FC-PR with 10% back reflection) and reamplified by the PM-EDFA back to +13 dBm. The back-propagated pulses are then combined with new laser pulses from the reference arm of FC-PBS1 in the in-loop FC-BOC. The in-loop FC-BOC measures the propagation delay change in the timing link and generates an error voltage. The error signal is processed by a proportional-integral (PI) controller and then applied to the fiber stretcher with a PZT amplifier (AMP) to compensate the fast timing jitter (see Fig. 1(c)). The piezo resonance of the stretcher at 18 kHz permits a closed loop bandwidth higher than 10 kHz. The output of the PI controller is also recorded by a data acquisition card (DAQ) so that when it reaches its output voltage limit, the motorized-delay is activated through a computer program serving as the slow compensation to the fluctuating link delay. Finally, the output of the FC-PR and the out-of-loop reference fiber are combined in FC-PBS2 and coupled into the out-of-loop FC-BOC to evaluate the performance of the link stabilization experiment.

In order to minimize the drifts coming from the length fluctuations in the FC-BOC reference paths, all setup elements are placed in a temperature-stabilized enclosure, except the 3.5-km fiber link spool, which is put outside and exposed to environmental fluctuations.

RESULTS AND DISCUSSION

Figure 2 shows the measured voltage responses of the FC-BOCs against the time delay between the incoming orthogonal pulses. Due to excess coupling loss between the PM fiber and the waveguide for the reverse-generated SH, the SH power collected on the forward path is approximately 10 dB higher than that of the reverse path in FC-BOCs. Therefore, a 10-dB attenuator is inserted to symmetrize the cross-correlation curve. This issue has prevented us from reaching higher timing sensitivities for FC-BOCs when compared with bulk optics cross-correlators. Nevertheless, even with the current coupling losses we have achieved comparable results to the previous work [5, 6]. For each FC-BOC, five different measurements are performed and the mean values of the jitter-to-voltage conversion factors are 4.5 mV/fs (± 0.32 mV/fs) and 82.0 mV/fs (± 4.9 mV/fs) for the in-loop and out-of-loop FC-BOC respectively (BPD transimpedance gain: 2×10^6 V/A, 3-dB bandwidth: 150 kHz, responsivity: 0.5 A/W).

ISBN 978-3-95450-134-2

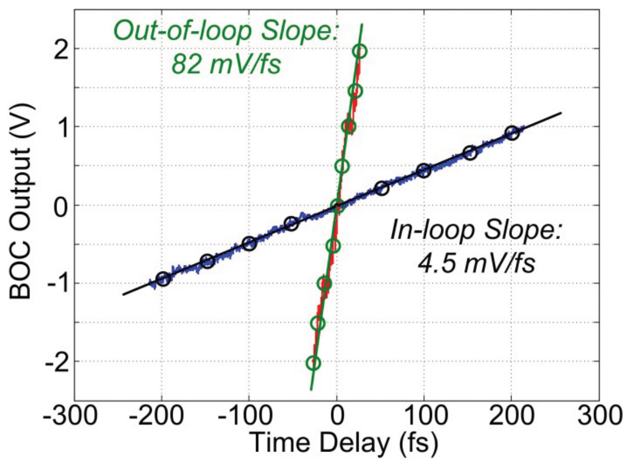

Figure 2: Measurement results of the FC-BOC output versus the delay between the pulses. Blue curve corresponds to the in-loop and red curve corresponds to the out-of-loop FC-BOC response.

The relative timing stability of the 3.5-km PM fiber link is continuously monitored for 200 hours without interruption. The black curve in Fig. 3(a) displays the residual timing drift measured by low-pass filtering the output of out-of-loop FC-BOC at 1 Hz (without any averaging). A remaining drift of only 3.3 fs (± 0.2 fs) RMS is measured for 200 hours of continuous link stabilization; and the motor delay has corrected for over 25-ps timing error. Relative temperature fluctuations of the 3.5-km fiber spool and the enclosure are plotted in Fig 3(b). The maximum deviation of the temperature is about 0.18 K and 0.06 K on the case of the fiber spool and inside the enclosure respectively. The correlation between the residual drift and the enclosure temperature confirms that the drift is mainly limited by the environmental fluctuations penetrating into the FC-BOCs. This is reasonable because the optical enclosure is large in volume, making it difficult to completely isolate the enclosed fibers from the laboratory environment. Even though we have spent considerable effort to splice as short fiber reference arms as possible, the system still contains in total ~2.5 m of uncompensated fiber (reference arms of the FC-BOCs and the fiber pigtail between FC-PR and FC-PBS2). A temperature fluctuation of ~0.1 K on 2.5-m uncompensated fiber would introduce ~7.5-fs error to the timing detection due to thermal expansion and contribute directly to the final drift. Hence, the observed residual drift in our experiment agrees well with the recorded relative temperature change.

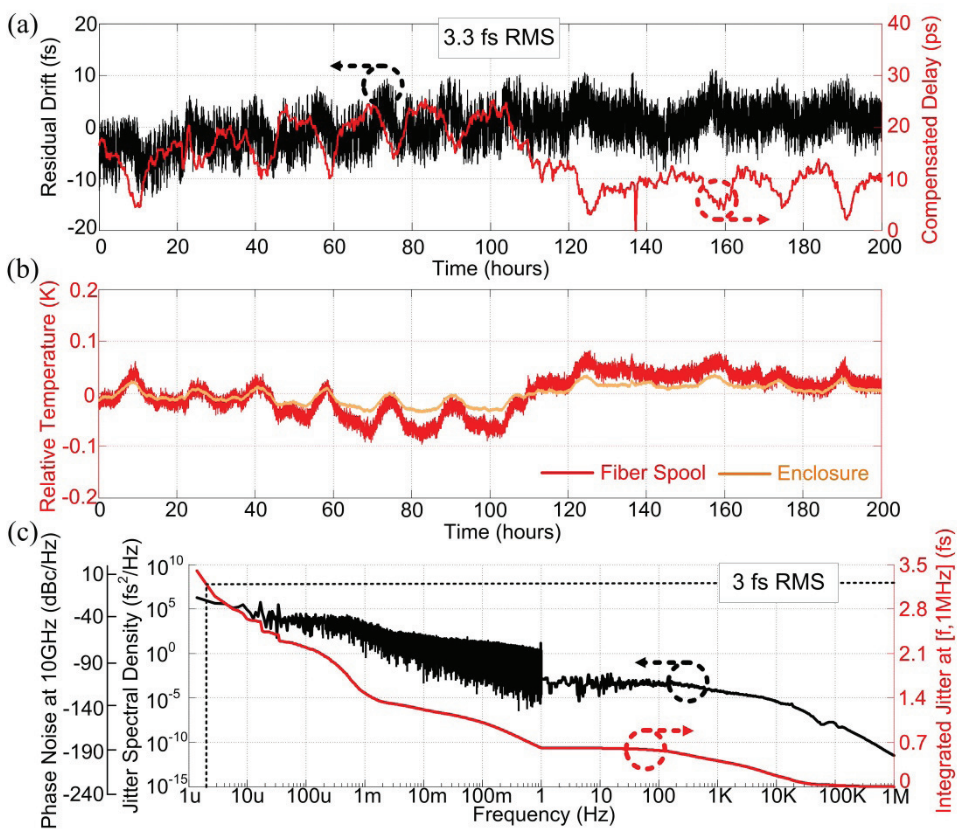

Figure 3: Out-of-loop measurement results. (a) Black curve: timing drift for 200 hours of continuous operation; red curve: corrected link propagation delay by the FC-MD. (b) Environmental conditions during the measurement, red curve: temperature measured on the 3.5-km fiber link spool; orange curve: temperature measured inside the enclosure. (c) Black curve: timing jitter spectral density and single-sideband phase noise (scaled at a 10 GHz carrier) from 1.4 µHz up to 1 MHz; red curve: its integrated jitter from frequency f up to 1 MHz.

ISBN 978-3-95450-134-2

The complete jitter spectral density of the link stabilization and its integrated jitter are shown in Fig. 3(c) (black and red curves respectively). The spectrum from 1 Hz up to 1 MHz is taken with a signal source analyzer (SSA) from the out-of-loop FC-BOC; whereas, the spectrum below 1 Hz is obtained by taking the Fourier transformation of the residual drift data shown in 3(a). The total jitter above 1 Hz is kept below 0.7 fs RMS, whereas the daily temperature fluctuations cause considerable jitter as can be seen from the frequency range below 1 mHz (red curve, Fig. 3(c)). Nevertheless, phase noise of only -20 dBc/Hz at an offset frequency of 2 μHz from a 10-GHz carrier is achieved and the total integrated jitter from 2 μHz up to 1 MHz is only 3 fs (± 0.18 fs) RMS which is more than sufficient for an efficient FEL synchronization.

CONCLUSION

In summary, we have successfully implemented a complete fiber-optic timing distribution system, which can be used for precise and long-term stable FEL synchronization.

We have demonstrated timing stabilization of a 3.5-km long fiber link using completely fiber-coupled elements. The out-of-loop measurement shows only 0.7-fs RMS link jitter integrated from 1 Hz to 1 MHz and 3.3-fs RMS residual drift below 1 Hz over 200 hours of continuous operation. Sub-fs precision over longer time intervals has been hampered by environmental fluctuations introducing timing detection errors via the uncompensated reference fiber arms. Local temperature stabilization of these reference arms would alleviate this effect and deliver better precision. Furthermore, the current efficiency of the FC-BOCs is limited by excess SH coupling loss, but still delivers a sensitivity comparable to the bulk-optic BOCs. The next generation device will include an integrated WDM to eliminate the coupling problem, thereby increasing the performance by an order of magnitude. Nevertheless, the current system based on FC-BOCs and PM fiber elements provides easy-to-implement, alignment-free, long-term stable, few-fs precision timing distribution under normal laboratory conditions. We believe that the demonstrated all-fiber timing distribution system can easily be deployed to an operating FEL, helping to both monitor and control electron bunch creation and fs X-ray pulse generation, to ultimately push the limits of spatially and temporally resolved imaging of molecular dynamics.

ACKNOWLEDGMENT

The authors acknowledge financial support by the Cluster of Excellence: The Hamburg Centre for Ultrafast Imaging-Structure, Dynamics and Control of Matter at the Atomic Scale of the Deutsche Forschungsgemeinschaft.

REFERENCES

[1] M. Altarelli, R. Brinkmann, M. Chergui, W. Decking, B. Dobson, S. Düsterer, G. Grübel, W. Graeff, H. Graafsma, and J. Hajdu, *XFEL: The European X-Ray Free-Electron Laser. Technical Design Report* (DESY, 2006).

[2] Stohr, J. Linac Coherent Light Source II (LCLS-II) Conceptual Design Report. No. SLAC-R-978. (SLAC, 2011).

[3] J. Kim, J. A. Cox, J. Chen, and F. X. Kärtner, "Drift-free femtosecond timing synchronization of remote optical and microwave sources," *Nature Photon.* **2**, 733-736 (2008).

[4] S. Schulz, I. Grguraš, C. Behrens, H. Bromberger, J. T. Costello, M. K. Czwalinna, M. Felber, M. C. Hoffmann, M. Ilchen, H. Y. Liu, T. Mazza, M. Meyer, S. Pfeiffer, P. Prędki, S. Schefer, C. Schmidt, U. Wegner, H. Schlarb, A. L. Cavalieri, "Femtosecond all-optical synchronization of an X-ray free-electron laser," *Nature Commun.* **6**, 6852 (2015).

[5] M. Y. Peng, P. T. Callahan, A. H. Nejadmalayeri, S. Valente, M. Xin, L. Grüner-Nielsen, E. M. Monberg, M. Yan, J. M. Fini, and F. X. Kärtner, "Long-term stable, sub-femtosecond timing distribution via a 1.2-km polarization-maintaining fiber link: approaching 10^{-21} link stability," *Opt. Express* **21**, 19982-19989 (2013).

[6] M. Xin, K. Şafak, M. Y. Peng, P. T. Callahan, F. X. Kärtner, "One-femtosecond, long-term stable remote laser synchronization over a 3.5-km fiber link," *Opt. Express* **22**, 14904-14912 (2014).

[7] M. Y. Peng, A. Kalaydzhyan, F. X. Kärtner, "Balanced optical-microwave phase detector for sub-femtosecond optical-RF synchronization," *Opt. Express* **22**, 27102-27111 (2014).

[8] A. J. Benedick, J. G. Fujimoto, and F. X. Kärtner, "Optical flywheels with attosecond jitter," *Nature Photon.* **6**, 97–100 (2012).

[9] A. H. Nejadmalayeri, F. N. C. Wong, T. D. Roberts, P. Battle, and F. X. Kärtner, "Guided wave optics in periodically poled KTP: quadratic nonlinearity and prospects for attosecond jitter characterization," *Opt. Lett.* **34**, 2522–2524 (2009).

[10] P. T. Callahan, K. Şafak, P. Battle, T. D. Roberts, F. X. Kärtner, "Fiber-coupled balanced optical cross-correlator using PPKTP waveguides," *Opt. Express* **22**, 9749-9758 (2014).

ISBN 978-3-95450-134-2